

## Fabrication of Porous Bioactive Glass-Ceramics via Decomposition of Natural Fibres

Pat SOOKSAEN<sup>1\*</sup>, Supakij SUTTIRUENGWONG<sup>1,2</sup>, Kunwadee ONIEM<sup>1</sup>,  
Khanamporn NGAMLAMIAD<sup>1</sup> and Jitlada ATIREKLAPWARODOM<sup>1</sup>

<sup>1</sup>Department of Materials Science and Engineering, Faculty of Engineering and Industrial Technology, Silpakorn University, Nakhon Pathom 73000, Thailand

<sup>2</sup>Center of Excellence for Petroleum, Petrochemicals and Advanced Materials, Silpakorn University, Nakhon Pathom 73000, Thailand

Received Sept. 22, 2008

Accepted Oct. 27, 2008

### Abstract

Porous bio glass-ceramics were prepared via natural fibres burning-out process. Glass-ceramics were fabricated by controlled crystallization of suitable glass compositions to give required crystalline phase/s. Porous structure was formed alongside during burning-out of natural fibres. Three glass batches were prepared in the SiO<sub>2</sub>-CaO-P<sub>2</sub>O<sub>5</sub>-K<sub>2</sub>O-Na<sub>2</sub>O-CaF<sub>2</sub> glass system, then melted, quenched and milled to give fine glass powders. DTA thermograms for the three glass compositions showed crystallization temperatures between 720 and 760°C and T<sub>g</sub> ranging between 508 and 645°C. Porous glass-ceramics were characterized for bulk density, phase evolution and microstructures. Different compositions resulted in different bulk densities and phases that crystallized out. Fluorapatite was found in all glass-ceramic samples, which indicated the biocompatibility and bioactivity and the potential future applications. Microstructures were also different from different heat-treated glass compositions, with more uniform pore size and shape in heat-treated samples containing a higher amount of Na<sub>2</sub>O and K<sub>2</sub>O.

**Key words** : Glass-ceramics, Heat-treatment, X-ray diffraction, Thermal analysis, Fluorapatite

### Introduction

Ceramics as potential materials for the reconstruction, fixation and repair of (the) diseased or broken parts of the musculo-skeletal system are known to possess properties such as bioinertia (e.g. alumina, zirconia), resorption (tricalcium phosphate), bioactivity (e.g. hydroxyapatite, bioactive glasses and glass-ceramics), or porosity for tissue ingrowth (hydroxyapatite-coated metals, alumina).<sup>(1-3)</sup> Tailoring the substrate compositions of bioactive ceramics leads to desired phases and properties. A large number of applications are at present available, including replacements for hips, knees, teeth, tendons and ligaments, and repair for periodontal disease, maxillofacial reconstruction, augmentation and stabilization of the jaw bone, spinal fusion, and bone fillers after tumor surgery.<sup>(1)</sup> Some ceramics even feature drug delivery potential and exhibit good biocompatibility. For specific types of application of bioceramics, microstructures consisting of macropores and micropores can increase the interfacial area between implant and tissues,

established in pores, leading to an increase in inertial resistance to movement of the device in the tissue.<sup>(1)</sup> However, when metals are mixed in the compositions, an undesired drawback on living tissues can occur. Hydroxyapatite (HAp) was used to overcome the above problem by coating on metals. Ducheyne et al. <sup>(4)</sup> reported the rate of bond formation in pores was sped up when HAp coated metal was applied. For the tissues to remain viable and healthy, pore sizes should be at least 100 to 150 μm in diameter to allow adequate supply of blood into the ingrowth connective tissue.<sup>(1)</sup> Interconnecting macropores and micropores and good pore size distribution are crucial factors for efficient transport of nutrient and food to the tissue ingrowth and promoting the osteointegration.<sup>(5)</sup>

Different compositions and treatments have recently been investigated for bioactive glasses and glass-ceramics.<sup>(6)</sup> Properties of bioglass and glass-ceramics formed are dependent on fabrication methods and the heat-treatment used.

---

\* Email: pat@su.ac.th

Pores of bioglass and glass-ceramics could be formed by addition of porogens, such as polymeric materials and foaming agents.<sup>(7)</sup> Rainer, et al.<sup>(8)</sup> prepared bioglass foams for mimicking bone tissue engineering using *in situ* foaming of a bioglass-loaded polyurethane foam as the intermediate step for obtaining a bioglass porous monolith. From this fabrication technique, the bioactive materials were prepared with three-dimensional processing and showed promising applications in reconstructive surgery tailored to each single patient.<sup>(8)</sup> Polyethylene glycol 4000 (HO (C<sub>2</sub>H<sub>4</sub>O) nH) with particles sizes of 5 and 500  $\mu\text{m}$  was used as foaming agent for preparing porous bioglass ceramic.<sup>(9)</sup> Lin and his group<sup>(9)</sup> reported the compatibility of porous bioglass ceramic with animal tissues. The microstructures of the implant were distributed uniformly in the material, which provided channels for bone ingrowth and improved the microscopic bioresorption.

Organic polymers are very attractive choices for generating desired pores and porosity due to the complete degradation at temperatures above 600°C. These organic polymers are rich in natural environment and are available as biomass such as dry and wet woods and crops. They can be obtained from wastes in many related industries such as food processing and wood finishing manufactures.

This paper aimed at preparing porous bioglass ceramics using natural fibres at different compositions as burning-out agent. The morphology of the materials and physical properties such as density and phases were also investigated.

## Materials and Experimental Procedures

### Preparation of Glass Powder

Three glass compositions were prepared according to Table 1. In each batch, raw materials were mixed thoroughly from appropriate ratios of silica sand (SiO<sub>2</sub> 99%), CaHPO<sub>4</sub> (Aldrich), K<sub>2</sub>CO<sub>3</sub> (Ajax), Na<sub>2</sub>CO<sub>3</sub> (Ajax) and CaF<sub>2</sub> (Aldrich) and then melted in alumina crucible at 1250°C for 2hrs followed by quenching in water at room temperature to retard crystallization, and milled to give fine glass powders. The compositions were chosen by fixing molar ratios of CaO and P<sub>2</sub>O<sub>5</sub> while changing the amount of network modifiers (Na<sub>2</sub>O and K<sub>2</sub>O). Differential Thermal Analysis

(DTA) was performed on glass powder from each batch using a Netzsch STA 449C (Germany) to record thermal transitions.

**Table 1.** Glass compositions melted in mol% oxide

Oxide	Glass I	Glass II	Glass III
SiO <sub>2</sub>	71.70	70.04	68.36
CaF <sub>2</sub>	11.95	12.11	12.25
K <sub>2</sub> O	4.07	4.11	4.15
Na <sub>2</sub> O	4.89	6.35	7.84
CaO	4.94	4.94	4.94
P <sub>2</sub> O <sub>5</sub>	2.45	2.45	2.45

### Preparation of Porous Glass-Ceramics

Natural fibre (wood dust) was ball milled and sieved through 180  $\mu\text{m}$  to yield fine particles suitable for further study as a burnt-out agent. The as-sieved wood dust was dried and studied for thermal decomposition by thermogravimetric analysis (TGA) using Perkin Elmer TAC7/DX. A fixed amount of wood dust (15 wt%) was mixed thoroughly with a fine glass powder from each batch using pestle and mortar. The mixture was then hydraulically pressed into pellets with a pressure of ~250 MPa for 20 seconds. The pellets had a diameter of 10 mm and thickness of ~10 mm. Heat-treatment was carried out at 800°C (following DTA data) for 2 hrs using a heating/cooling rate of 3°C/min to form porous bioactive glass-ceramics. Several heat-treated samples were made and then calculated for bulk density using a 4-digit precision balance.

### Characterization

X-ray diffraction (XRD) was used to identify phases present in the glass-ceramics. Before the analysis, samples from each composition were crushed into fine powder. The analysis was then performed on a Bruker AXS D8 Advance Diffractometer with a scan speed of 2°/min and step size 0.02° using Cu K $\alpha$  radiation with a wavelength of  $\lambda = 1.5406 \text{ \AA}$ . For microstructural analysis, glass-ceramic samples were fractured and chemically etched using concentrated HF (50%) 20 ml, concentrated HNO<sub>3</sub> (70%) 5 ml and deionized water 75 ml in order to

*Fabrication of Porous Bioactive Glass-Ceramics  
via Decomposition of Natural Fibres*

reveal microstructures. Etching was carried out at room temperature for 1 minute. Samples were then gold coated by a Cressing Sputter Coater 108 for Scanning Electron Microscope (SEM). Analysis was carried out using a Camscam with EDAX link operated at 10 – 20 kV. Backscattered electron (BE) mode was used to reveal microstructures and observe qualitative changes in composition at the sample surface.

## Results and Discussion

Quenching the glass melt in water at room temperature resulted in translucent material for all three compositions. After ball milling, a fine white glass powder was obtained in each composition. The translucency might have occurred due to partial crystallization during quenching or due to incomplete melting of the glass batch.<sup>(12-14)</sup> However, fine glass powders in this study were able to crystallize to form bioactive glass-ceramics at a later stage.

Thermal analysis of wood particles by TGA (not shown) as reported elsewhere<sup>(10, 11)</sup> revealed a first decomposition range at temperatures below 250 °C, which was possibly due to dehydration and primary devolatilization of hemicellulose and lignin during heating. On further heating there was a secondary devolatilization, eventually leading to tar formation.

DTA traces of glasses I, II and III are shown in Figures. 1, 2 and 3, respectively. The thermal transitions were detected and recorded by computer software equipped with a Netzsch STA 449C DTA. The first endotherm from each glass composition was detected from the slope change of derivative curve (DDTA) and corresponds to the glass transition temperature,  $T_g$ . It was found that glass containing a higher amount of  $\text{Na}_2\text{O}$  as network modifier resulted in lower  $T_g$ . The  $T_g$  values were 645, 535 and 508°C for glasses I, II and III, respectively. Exotherms in all three compositions can be correlated with the crystallization of glasses to form glass-ceramics. These exotherms were in the temperature range of 700 – 780°C. Therefore in this study, heat-treatment was performed at 800°C (following DTA data) to form porous glass-ceramics, assuming phase evolution was completed at this temperature.

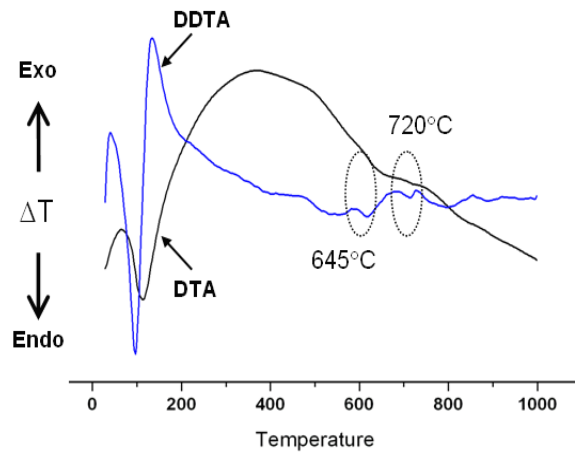


**Figure 1.** DTA and DDTA traces of as-quenched glass I

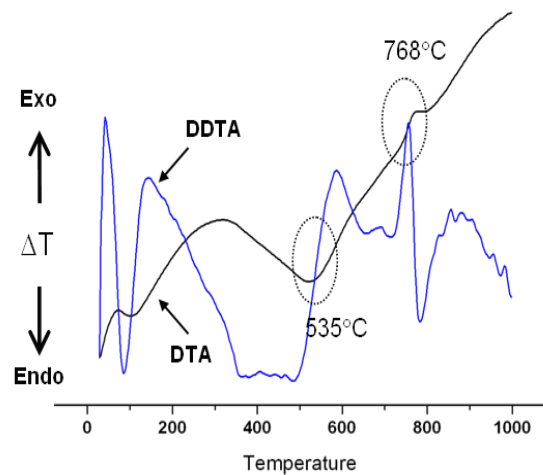


**Figure 2.** DTA and DDTA traces of as-quenched glass II

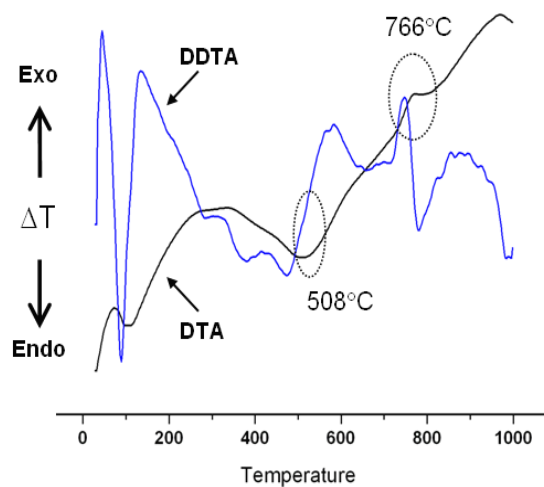


**Figure 3.** DTA and DDTA traces of as-quenched glass III

As far as bulk density of porous glass-ceramics was concerned, it was found that on addition of 15 wt% burning-out agent, glass-ceramic I resulted in the highest average bulk density at 1.59 gcm<sup>-3</sup> followed by glass-ceramic II (0.80 gcm<sup>-3</sup>) and glass-ceramic III (0.64 gcm<sup>-3</sup>). The difference in bulk density shown in Figure.4 may have been the consequence of the effect of different types and amounts of crystals and also different pore sizes present in the glass-ceramic samples.

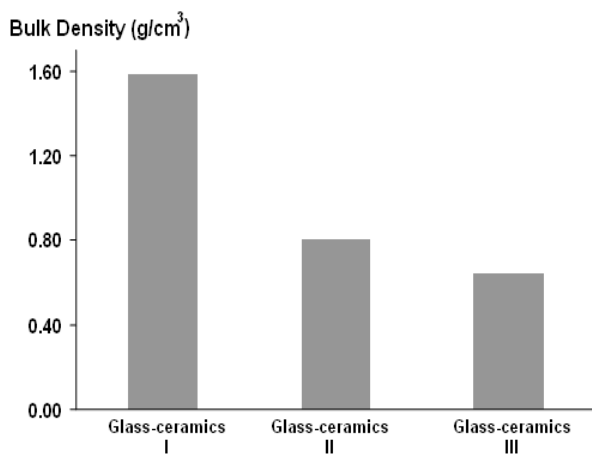


**Figure 4.** Bulk density of porous glass-ceramics with 15 wt% wood dust

XRD traces of heat-treated glasses I, II and III with 15 wt% burntout are shown in Figure5. There are various peaks from different phases overlapped. Fluorapatite (JCPDS card number 15-876) which is responsible for the bioactivity<sup>(12, 13)</sup> was found in all glass-ceramic samples. Therefore these materials have potential biomedical applications such as fillers and bone replacement. However, the bioactivity and biocompatibility of these materials should be further investigated. In glass-ceramic composition I (Figure 5a), in addition to fluorapatite, large amount of tridymite was also crystallized out possibly due to a higher amount of SiO<sub>2</sub> in the glass batch. Some tiny peaks responsible for sanidine (KAlSi<sub>3</sub>O<sub>8</sub>) were also detected in this sample. In compositions II and III (Figures 5b, 5c), peaks responsible for sanidine were clearly seen, indicating a larger amount of this phase crystallized out from these samples. In addition, calcite was another phase detected in glass-ceramic composition III.

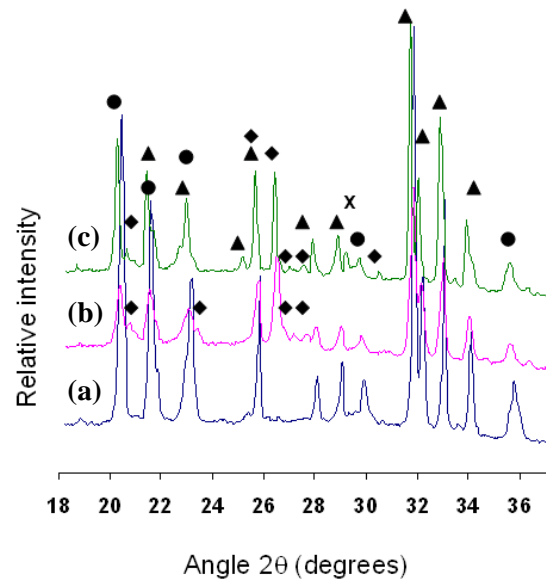


**Figure 5.** XRD traces of glass-ceramics with 15 wt% wood dust (a) glass-ceramic I, (b) glass-ceramic II and (c) glass-ceramic III  
 ● Tridymite SiO<sub>2</sub> ▲ Fluorapatite Ca<sub>5</sub>(PO<sub>4</sub>)<sub>3</sub>F  
 ◆ Sanidine K(AlSi<sub>3</sub>O<sub>8</sub>) × Calcite CaCO<sub>3</sub>

Microstructures of porous glass-ceramics are shown in Figures 6a-6c. for glass-ceramic I, II and III, respectively. It can be seen under the same magnification that the porous structures were different. In glass-ceramic I, pore shape, size and distribution were not uniform. The largest pore size was ~600 μm and the smallest ones were ~100 μm, all distributed randomly throughout the structure. In glass-ceramic II, the pore shape was spherical and the size was larger than that in glass-ceramic I. The open pores were uniformly distributed and formed sponge-like. These large pore sizes varied from 600 - 700 μm. Microstructure from glass-ceramic III was similar to that of glass-ceramic II; however, the pore size was larger in general and varied from 800 - 1200 μm (Figures 6b and 6c). The dependence of pore sizes and glass-ceramic formulations was not clearly observed. However, microstructural analysis revealed that the lower value of bulk density resulted from larger pore size. The explanation was not so far known but could have been that glass-ceramic III had a larger amount of Na<sub>2</sub>O as a network modifier and smallest amount of SiO<sub>2</sub>, hence reduced the viscosity of glass above T<sub>g</sub>. Reduced viscosity of glass-ceramic III may have caused wood dust to agglomerate in some areas, leaving larger pores after crystallization at 800°C. In addition to that, considering when the heat treatment temperature increased, wood dust started to degrade and

*Fabrication of Porous Bioactive Glass-Ceramics  
via Decomposition of Natural Fibres*

gradually turned to carbonaceous compounds. These more hydrophobic particles of degraded wood dust may have attracted and given rise to the larger pore sizes. Thus, the colours of glass-ceramics II and III were darker than that of glass-ceramic I (results not shown).

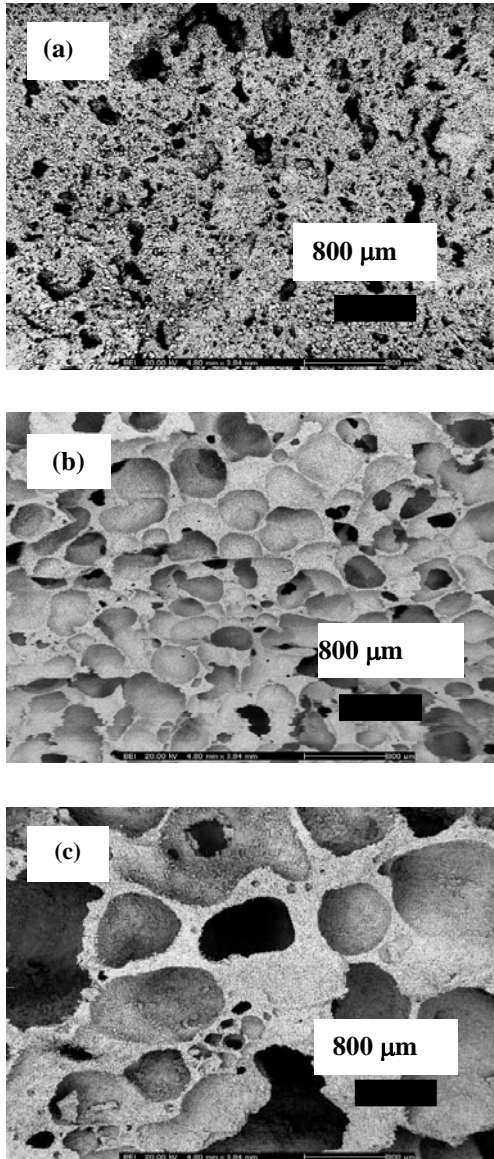


**Figure 6.** SEM images (BEI mode) of glass-ceramics with 15 wt% wood dust (a) glass-ceramic I, (b) glass-ceramic II and (c) glass-ceramic III

Higher magnification SEM images of glass-ceramic I are shown in Figure 7. Three crystal types were observed as indicated in Figures 7a and 7b. Energy dispersive spectroscopy analysis (Figure 8) found needle-like crystals in Figure 7b

composed mainly of Ca and P. Therefore they may be correlated with the fluorapatite phase,  $\text{Ca}_5(\text{PO}_4)_3\text{F}$ , which is bioactive. Peaks for Na, Al, Si and K may have formed due to contamination from surroundings. An Au peak comes from gold sputtering during sample preparation. Figure 9 shows a higher magnification SEM image of glass-ceramic II, in which three crystal types were observed. It may be correlated with three phases found by XRD. Chemical analysis on a long needle-like crystal in Figure 9b, also detected mainly Ca and P which could also be responsible for the fluorapatite phase. The bioactivity of these porous glass-ceramics is of substantial concern and this will be carried out *in vitro* using stimulated body fluid (SBF) in the next step of the research, which should then examine the feasibility of using them as bio-implant materials.

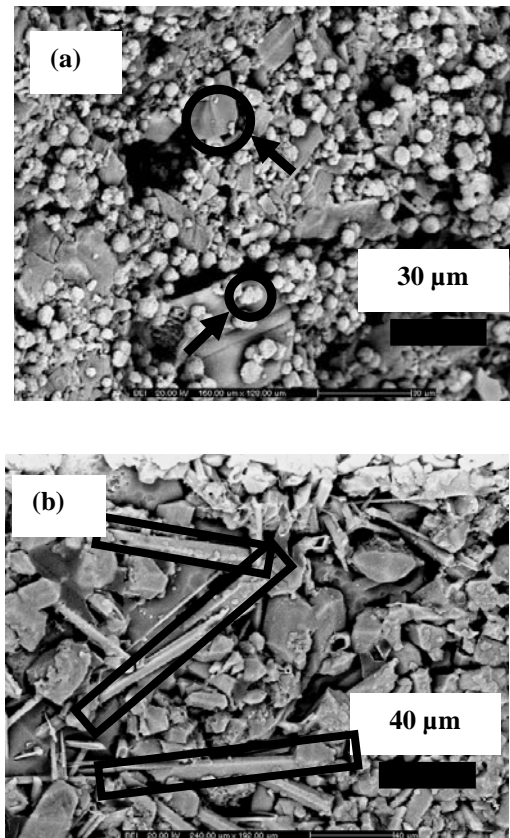


**Figure 7.** Higher magnification SEM images (BEI mode) of glass-ceramic I with 15 wt% wood dust (a) area showing large (marked by large circle) and small rounded crystals (marked by small circle) and (b) area showing needle-like crystals (marked by open rectangles)

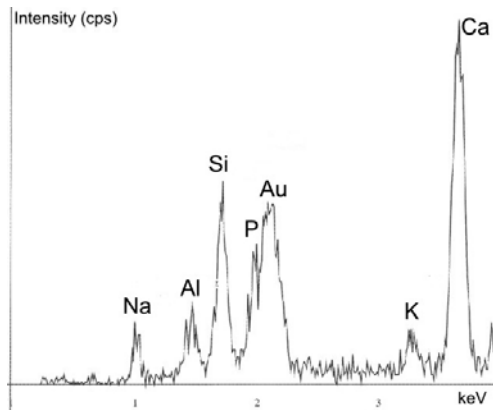


**Figure 8.** EDS analysis on a needle-like crystal

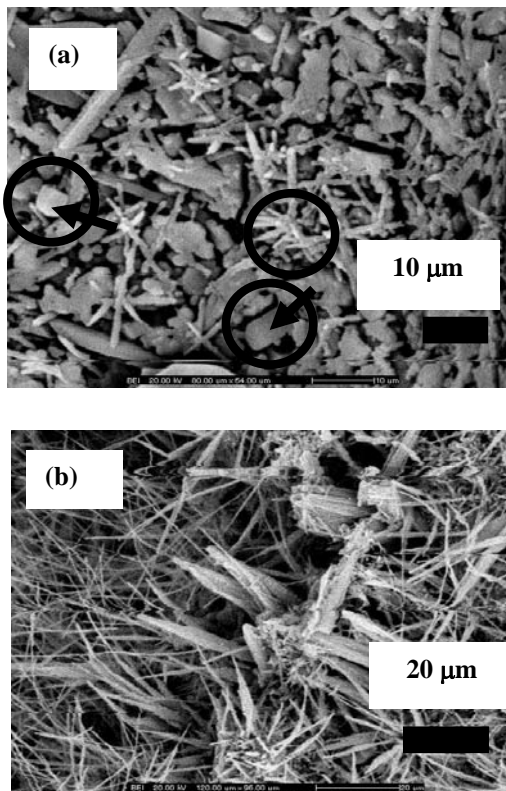


**Figure 9.** Higher magnification SEM images (BEI mode) of glass-ceramic II with 15 wt% wood dust (a) area showing fine needles (in circle), large and small rounded crystals (in circle and arrow indicated) and (b) an area with long needle-like crystals

## Conclusions

Wood dust can be used as a burntout agent in the fabrication of porous glass-ceramics. As-quenched glasses showed translucency probably as a result of partial crystallization and/or incomplete

reaction during glass melting. Heat-treatment for 2 hrs at 800°C resulted in crystallization of fluorapatite, the bioactive phase, in all compositions. Different phases other than fluorapatite were also found in different heat-treated samples. It was found that bulk density decreased as the amount of network modifiers ( $\text{Na}_2\text{O}$  and  $\text{K}_2\text{O}$ ) in the glass batch composition increased. Microstructural analysis showed larger pore size in samples containing a higher amount of network modifiers.

## Acknowledgements

The authors would like to thank the department of Materials Science and Engineering, Silpakorn University and the Center of Excellence for Petroleum, Petrochemicals and Advanced Materials, for financial support as well as Mr Sittichoke Chaiwan, Department of Ceramics, Silpakorn University, for help in ceramic processing.

## References

1. Hench, L. L. 2005. Bioceramics: From concept to clinic. *J. Am. Ceram. Soc.* **74** : 1487–1510.
2. Hench, L.L. 1991. *J. Am. Ceram. Soc.* **74(7)** : 1487 -1510.
3. Holand, W, J. 1997. Biocompatible and bioactive glass-ceramics-state of the art and new directions. *J. Non-Cryst. Solids.* **219** : 192-197.
4. Ducheyne, P. J. 1985. *Biomed. Mater. Res.* **19** : 273-91.
5. Fidancevska, E., Ruseska, G., Bossert, J., Lin, Y.M. and Boccaccini, A.R. 2007. Fabrication and characterization of porous bioceramic composites based on hydroxyapatite and titania. *Mater. Chem. Phys.* **103(1)** : 95-100.
6. Salinas, A.J., Roman, J., Vallet-Regi, M., Oliveira, J.M., Correia, R.N. and Fernandes, M.H. 2000. In vitro bioactivity of glass and glass-ceramics of the  $3\text{CaO-P}_2\text{O}_5\text{-CaO-SiO}_2\text{-CaO-MgO-2SiO}_2$  system. *Biomaterials* **21(3)** : 251-257.

*Fabrication of Porous Bioactive Glass-Ceramics  
via Decomposition of Natural Fibres*

7. Karlsson, K.H., Ylänen, H. and Hannu, A. 2000. Porous bone implants. *Ceram. Int.* **26(8)** : 897-900.
8. Rainer, A., Giannitelli, S.M., Abbruzzese, F., Traversa, E., Licoccia, S. and Trombetta, M. 2008. Fabrication of bioactive glass-ceramic foams mimicking human bone portions for regenerative medicine. *Acta Biomater.* **4(2)** : 362-9.
9. Lin, F.-H., Huang, Y.-Y., Hon, M.-H. and Wu, S.-C. J. 1991. Fabrication and biocompatibility of a porous bioglass ceramic in a  $\text{Na}_2\text{O}$ -- $\text{CaO}$ -- $\text{SiO}_2$ -- $\text{P}_2\text{O}_5$  system. *J. Biomed. Eng.* **13(4)** : 328-334.
10. [Http://www.chamotlabs.com/ApplicationNotes/HTC/HTC34thmidwest.html](http://www.chamotlabs.com/ApplicationNotes/HTC/HTC34thmidwest.html).
11. [Http://www.fpl.fs.fed.us/documnts/pdf2001/white01a.pdf](http://www.fpl.fs.fed.us/documnts/pdf2001/white01a.pdf).
12. Agathopoulos, S., Tulyaganov, D.U., Marques, P.A.A.P., Ferro, M.C., Fernandes, M.H.V. and Correia, R.N. 2003. The fluorapatite-anorthite system in biomedicine. *Biomaterials.* **24(7)** : 1317–1331.
13. Chen, X, Hench, L.L., Greenspan, D., Zhong, J., Zhang, X. 1998. Investigation on phase separation, nucleation and crystallization in bioactive glass-ceramics containing fluorophlogopite and fluorapatite. *Ceram. Int.* **24** : 401-410.
14. James, P.F. 1995. Glass ceramics : new compositions and uses. *J. Non-Cryst. Solids.* **181** : 1-15.
15. Peitl, O., Zanotto, E.D., Hench, L.L. 2001. Highly bioactive  $\text{P}_2\text{O}_5$ - $\text{Na}_2\text{O}$ - $\text{CaO}$ - $\text{SiO}_2$  glass-ceramics. *J. Non-Cryst. Solids.* **292(1-3)** : 115-126.
16. Duan, R.-G., Liang, K.-M. and Gu, S.-R. 1999. The effect of additives on the crystallization of  $\text{Na}_2\text{O}$ - $\text{CaO}$ - $\text{MgO}$ - $\text{Al}_2\text{O}_3$ - $\text{SiO}_2$ - $\text{YiO}_2$  system glasses. *J. Mater. Proc. Technol.* **87(1-3)** : 192–197.